

## Coupled double-layer Fano resonance photonic crystal filters with lattice-displacement

Yichen Shuai, Deyin Zhao, Arvinder Singh Chadha, Jung-Hun Seo, Hongjun Yang, Shanhui Fan, Zhenqiang Ma, and Weidong Zhou

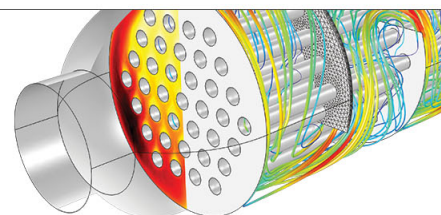
Citation: *Applied Physics Letters* **103**, 241106 (2013); doi: 10.1063/1.4846475

View online: <http://dx.doi.org/10.1063/1.4846475>

View Table of Contents: <http://scitation.aip.org/content/aip/journal/apl/103/24?ver=pdfcov>

Published by the AIP Publishing

Over **700** papers &  
presentations on  
multiphysics simulation



VIEW NOW ►

 COMSOL

# Coupled double-layer Fano resonance photonic crystal filters with lattice-displacement

Yichen Shuai,<sup>1</sup> Deyin Zhao,<sup>1</sup> Arvinder Singh Chadha,<sup>1</sup> Jung-Hun Seo,<sup>2</sup> Hongjun Yang,<sup>1,3</sup> Shanhui Fan,<sup>4</sup> Zhenqiang Ma,<sup>2</sup> and Weidong Zhou<sup>1,a)</sup>

<sup>1</sup>Department of Electrical Engineering, University of Texas at Arlington, Arlington, Texas 76019, USA

<sup>2</sup>Department of Electrical and Computer Engineering, University of Wisconsin, Madison, Wisconsin 53706, USA

<sup>3</sup>Semerane, Inc., Arlington, Texas 76010, USA

<sup>4</sup>Department of Electrical Engineering, Stanford University, Stanford, California 94305, USA

(Received 22 October 2013; accepted 26 November 2013; published online 10 December 2013)

We present here ultra-compact high-Q Fano resonance filters with displaced lattices between two coupled photonic crystal slabs, fabricated with crystalline silicon nanomembrane transfer printing and aligned e-beam lithography techniques. Theoretically, with the control of lattice displacement between two coupled photonic crystal slabs layers, optical filter Q factors can approach 211 000 000 for the design considered here. Experimentally, Q factors up to 80 000 have been demonstrated for a filter design with target Q factor of 130 000. © 2013 AIP Publishing LLC. [<http://dx.doi.org/10.1063/1.4846475>]

In recent years, great interests have been attracted to single layer ultra-compact surface-normal nanostructured optical filters and reflectors<sup>1–9</sup> mostly based on one-dimensional high contrast gratings (1D HCGs)<sup>6,10</sup> and two-dimensional photonic crystal slabs (2D PCSs).<sup>4,8,9,11</sup> The phase matching, provided by in-plane periodic index modulation, enables the coupling of guided modes with out-of-the-plane radiations, resulting in Fano interference and guided mode resonance (GMR) effects.<sup>1,2,12,13</sup> Extremely high quality factor (Q) optical filters can be obtained in these structures with asymmetric resonance lineshapes due to Fano interference effect, which creates a sharp transition between transmission peak and dip.<sup>13</sup> Optical filters based on single layer 2D PCSs have been investigated extensively.<sup>3,5,14–20</sup> However, single layer PCS Fano filters offer limited dispersion engineering capabilities for fine-tuning the output spectrum.

Coupled bi-layer PCS structures, on the other hand, were proposed and reported to have very high Q factors and strong optomechanical forces.<sup>21,22</sup> Suh *et al.* and Liu *et al.* reported previously that optical Q-factors and optomechanical interactions can be controlled by precisely tuning the gap and the lattice displacement between two coupled PCS.<sup>14,23</sup> When considered theoretically, one can achieve infinite Q factors in the dark states arising from coupled bright or dark resonances in symmetric or asymmetric coupled bi-layer PCSs, respectively.<sup>23</sup> Using single step e-beam lithography patterning processes, researchers have experimentally demonstrated coupled bi-layer PCS structures in InP material systems, with strong optomechanical interactions and modest Q factors ( $\sim 1600$ ).<sup>24</sup> We also reported that coupled double-layer Fano resonance PCS filters with experimentally demonstrated Q factor of 9734 and extinction ratio of 8 dB, for a filter design with a target Q of 22 000.<sup>25</sup> In Refs. 24 and 25, the lattices of holes in the two layers are aligned with respect to each other. It was established theoretically that allowing lateral displacement of the lattices in the two layers with

respect to each other would enable an additional degree of freedom in the control of the filter characteristics of the two-layer structure.<sup>14,23</sup> However, experimental demonstration of coupled double-layer PCS structures with controlled lattice displacement has not been reported due to the challenges associated with its fabrication. Employing PDMS (polydimethylsiloxane) nanomembrane transfer printing technique, it is possible to stack multi-layers of semiconductor and other dielectric materials.<sup>8,26</sup> We report here the design and experimental demonstration of coupled double-layer PCS with precisely controlled lattice displacement, based on transfer printing and multi-layer e-beam patterning alignment processes.<sup>26,27</sup> Both simulation and measurement suggest that optical filter Q factors are very sensitive to the lattice displacement. For one structure with relatively large lattice displacement, we demonstrated a Q factor of 80 000 experimentally. Further design and process optimization lead us to expect much higher Q-factors with a simulation Q

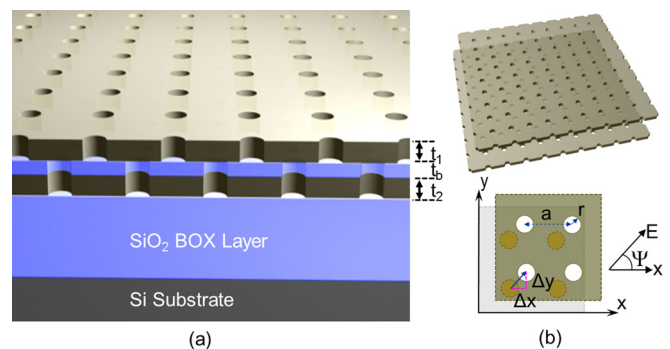


FIG. 1. (a), (b) Schematics of Fano resonance filters based on PDMS transfer printed coupled double layer photonic crystal slab (nanomembrane) on silicon substrate. (a) 3D close-up view with lattice displacement and thin oxide buffer layer ( $t_0$ ) sandwiched in between two single layer crystalline silicon PC layers ( $t_1$  and  $t_2$ ); (b) illustration and definition of key design parameters, including lattice constant ( $a$ ), air hole radius ( $r$ ), and lattice displacement ( $\Delta x$ ,  $\Delta y$ ) between two layers. The inset shows the incident beam polarization ( $E$ -vector)  $\Psi$  definition.

<sup>a)</sup>wzhou@uta.edu

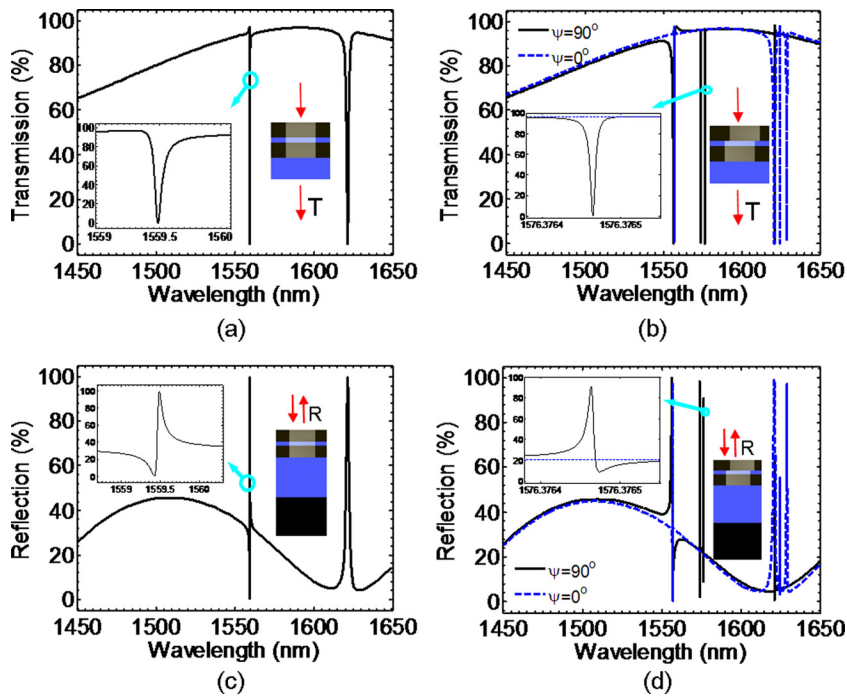


FIG. 2. Simulated transmission and reflection spectra for double layer stacked Fano filters (a), (c) without and (b), (d) with lattice offset ( $\Delta x = 0.2a$ ,  $\Delta y = 0.5a$ ), with the insets shown the zoom-in plot for the dominant (high Qs) resonance for each cases. Also shown in the insets are the schematics of the structures considered in the simulation. For the transmission spectra shown in (a), (b), glass substrate was considered. For the reflection spectra shown in (c), (d), SOI substrate was considered.

factor of  $2.11 \times 10^8$  for coupled double-PCS structures with optimal lattice displacement.

The optical filter is shown schematically in Fig. 1, where two single layer PCSs (with thicknesses  $t_1$  and  $t_2$ ) are stacked with controlled lattice displacement ( $\Delta x$ ,  $\Delta y$ ). An ultra-thin low index oxide buffer layer (with thicknesses  $t_b$ ) is sandwiched in between, serving as the coupling layer. A square lattice PCS structure was used here with air hole radius ( $r$ ) and lattice period ( $a$ ). The filter transmission and reflection spectra were computed using the Fourier Modal Method with a freely available Stanford Stratified Structure Solver ( $S^4$ ) software package.<sup>28</sup> Here we consider surface-normal incident beams for the filter design and measurement. The incident beam polarization (E-vector)  $\Psi$  is defined as the angle from the positive x-axis to the polarization direction, as shown in the inset of Fig. 1(b).

The design parameters are chosen based on the structure reported earlier,<sup>25</sup> with  $a = 1000$  nm,  $r/a = 0.08$ ,  $t_1 = t_2 = 230$  nm,  $t_b = 20$  nm. Simulations were carried out to find the Q factors for different lattice displacements ( $\Delta x$ ,  $\Delta y$ ). Shown in Fig. 2 are simulated transmission and reflection spectra for double layer stacked Fano filters without (Figs. 2(a) and 2(c)) and with (Figs. 2(b) and 2(d)) lattice offset ( $\Delta x = 0.2a$ ,  $\Delta y = 0.5a$ ), with the insets showing the zoom-in plot for the dominant (highest Q) resonance in each case. Also shown in the insets are the schematics of the structures utilized in the simulation. The transmission spectra shown in Figs. 2(a) and 2(b) used a glass substrate. The reflection spectra shown in Figs. 2(c) and 2(d) used a SOI substrate. The results shown in Figs. 2(b) and 2(d) correspond to the highest Q value obtained for this set of design parameters. Notice that Fano filter Q increases from 26 000 and 28 000 for the

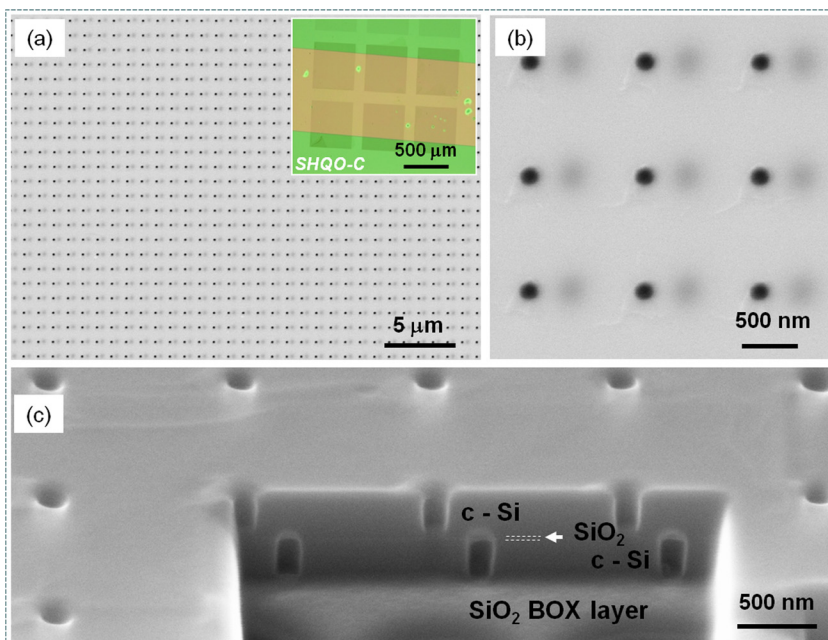


FIG. 3. Fabricated Fano filter SEM images: (a) top view; (b) zoom-in top view, and (c) cross-sectional view of double layer Fano filter on SOI, with controlled lattice misalignment offset ( $\Delta x = 0.2a$ ,  $\Delta y = 0$ ). Shown in the inset of (a) is a micrograph showing multiple device structures with top and bottom PCS pattern areas.

perfectly aligned lattice structures (Figs. 2(a) and 2(c)) to  $2.11 \times 10^8$  and  $1.76 \times 10^8$  for the lattice misaligned structures (Figs. 2(b) and 2(d)) with an optimal lattice displacement of  $\Delta x = 0.2a$  and  $\Delta y = 0.5a$ . It is also worth mentioning that the low index buffer layer (e.g.,  $\text{SiO}_2$  used here) thickness can also be varied for Q-factors approaching infinity.<sup>23,25</sup>

A thin oxide buffer layer ( $t_b = 20$  nm in this case) was first formed by thermal oxidation of a single crystalline Si layer on a SOI substrate, followed by the definition of Cr/Au global alignment marks based on e-beam lithography (EBL) and the metal lift-off processes. The bottom PCS structure was then formed by a 2nd EBL patterning, aligned with the Cr/Au global alignment marks, and reactive-ion etching (RIE) dry etching processes. A piece of single crystalline Si nanomembrane (1 mm  $\times$  2 mm size) was released from another unpatterned SOI substrate and stacked onto the patterned bottom PCS SOI substrate using the PDMS transfer printing process.<sup>8,26</sup> A 3rd EBL step was used to pattern the top PCS layer, aligned with the same global alignment marks, with alignment accuracy  $\sim 10$  nm.

With the control of the pattern location, we achieved precise control of lattice displacement between top and bottom PCS layers. Shown in Fig. 3 are scanning electron microscope (SEM) images of fabricated double layer PCS Fano filters with displaced lattices between coupled PCS layers. The cut-out cross-sectional view SEM image shown in Fig. 3(c) was prepared with the focused ion beam (FIB) technique. Clearly, coupled double-layer PCS structures with oxide buffer were achieved using precisely controlled lattice displacement ( $\Delta x = 0.2a$ ,  $\Delta y = 0$ ). Also shown in the inset of Fig. 3(a) is a microscopic image of coupled double layer PCS optical filters with six patterned device structures (bottom squares) and patterned top PCS structures on a piece of transferred crystalline Si nanomembrane.

The Fano filters were characterized by measuring the reflection spectra with an Agilent tunable laser system with 1 pm resolution and 9 dBm output power. The incident beam goes through an optical circulator, a laser beam collimator, an optical lens, a linear polarizer, and a beam splitter. Selected results with  $\Psi = 0^\circ$  are shown in Figs. 4 and 5 for two cases with relatively small and large lattice displacements, respectively. For the small lattice displacement case shown in Fig. 4, the lattice offsets are  $\Delta x = 0.045a$  and  $\Delta y = 0.015a$ , obtained based on the estimate from the top view SEM image shown in the inset of Fig. 4(a). Measured resonance was also simulated based on  $S^4$  package and fitted with Fano resonance formula.<sup>29</sup> The results are shown in Fig. 4(b) for the zoom-in plot of the dominant resonance at 1549 nm. Fig. 4(c) shows the simulation spectra for two orthogonal polarization directions  $\Psi = 0^\circ$  and  $90^\circ$ . The actual lattice parameters used in the simulation here are  $a = 1000$  nm,  $r/a = 0.091$ , and  $t_1 = 227$  nm,  $t_2 = 230$  nm, and  $t_b = 23$  nm, based on SEM images from the fabricated device. These fine adjustments in lattice parameters are well within the fabrication tolerances. The results agree very well (Fig. 4(b)). Comparing to the simulated Q of 16 000, we obtained measured Q factor of 11 500 with 5.5 dB extinction ratio (ER), defined as the ratio between the peak and the dip at Fano resonance. The other peak at 1569 nm shown in Fig. 4(a) is less prominent, and we did not consider this one here.

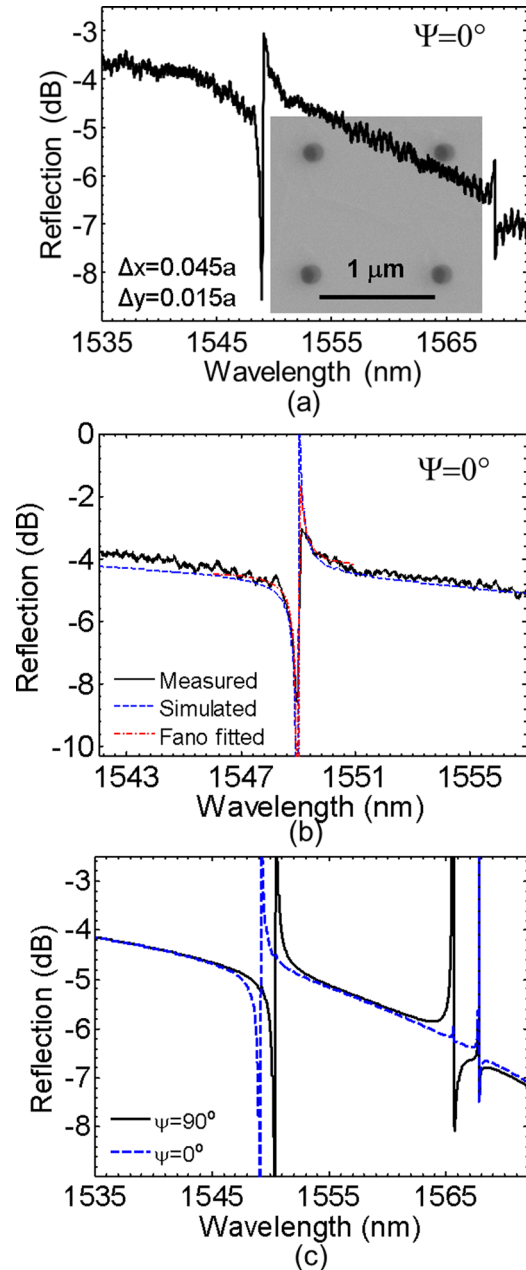


FIG. 4. (a) Measured reflection spectra at  $\Psi = 0^\circ$  for a displaced Fano filter with very small offset ( $\Delta x = 0.045a$ ,  $\Delta y = 0.015a$ ), with a top view SEM image shown in the inset; (b) zoom-in plots around the dominant resonance with measured (black solid line), simulated (blue dashed line), and Fano fitted (red dashed line) reflection spectra; and (c) simulation spectra for two polarization angles  $\Psi = 0^\circ$  (blue dashed line) and  $\Psi = 90^\circ$  (black solid line) based on the fabricated device parameters.

This case is very similar to the results we reported earlier for coupled double-layer PCS filters without lattice displacement.<sup>25</sup>

Since the optical Q factors are very sensitive to the lattice displacement, we expect much higher Q factors to be obtained for a different set of lattice displacements. Shown in Fig. 5 are the results obtained for the coupled double layer PCSs, with large lattice displacement ( $\Delta x = 0.495a$ ,  $\Delta y = 0.45a$ ). The measured reflection spectrum ( $\Psi = 0^\circ$ ) is shown in Fig. 5(a), with top-view SEM image shown in the inset. We obtained two resonant locations, around 1548.6 nm and 1567 nm. The zoom-in plot around 1548.6 nm resonant is shown in Fig. 5(b) with simulation and Fano fitted spectra.



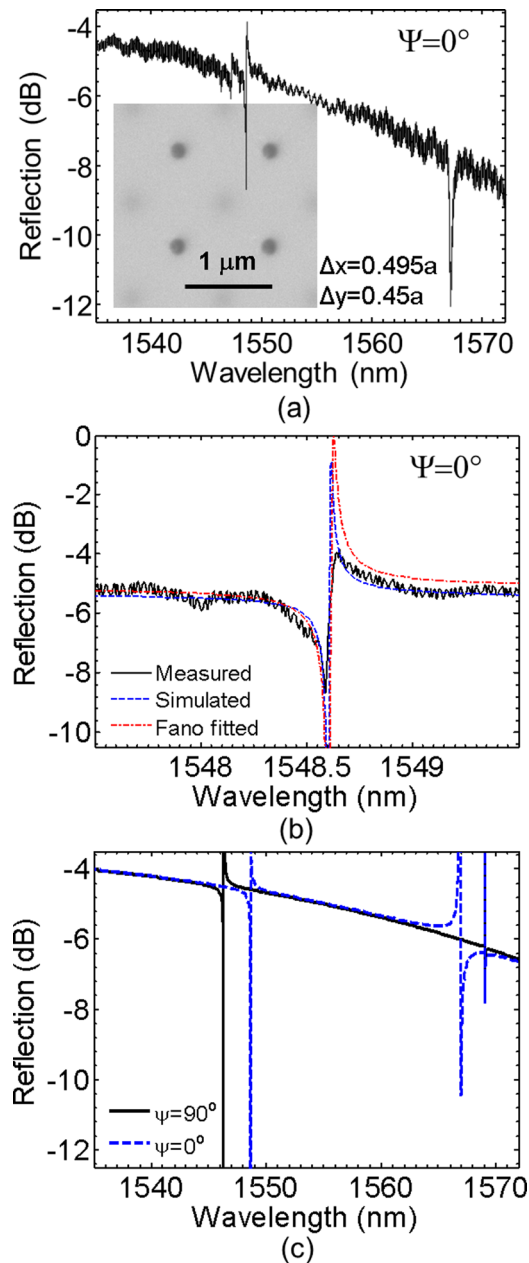


FIG. 5. (a) Measured reflection spectra at  $\Psi=0^\circ$  for a displaced Fano filter with large offset ( $\Delta x=0.495a$ ,  $\Delta y=0.45a$ ), with a top view SEM image shown in the inset; (b) zoom-in plots around the dominant resonance with measured (black solid line), simulated (blue dashed line), and Fano fitted (red dashed line) reflection spectra; and (c) simulation spectra for two polarization angles  $\Psi=0^\circ$  (blue dashed line) and  $\Psi=90^\circ$  (black solid line) based on the fabricated device parameters.

Fig. 5(c) shows the simulation spectra for the same lattice displacement. The lattice parameters used in the simulation here are  $a=1000$  nm,  $r/a=0.086$ , and  $t_1=228$  nm,  $t_2=230$  nm, and  $t_b=23.2$  nm, based on SEM images from the fabricated device. In this case of larger lattice displacement, we obtained a measured Q factor of 80 000, with simulated Q factor of 130 000 for this case. This measured Q value is the highest experimental Q factor reported out of all the cases we fabricated. The reduction in the measured Q values and relatively small ERs may be related to the fabrication imperfections (e.g., sidewall straightness and roughness and pattern uniformity). Additionally, the use of the focused laser beam (though an objective lens) may also

impact the measured Q and ER values as Fano resonance based filters are very sensitive to the incident angles. All simulations are based on surface-normal incident beam with perfectly collimated light beam. We noticed that the (focused) incident beam can affect the measured spectral output, with much more profound effect for very high Q factor measurement. We anticipate much higher Q-factors can be obtained with precisely controlled displacement, optimized fabrication process, and improved measurement setup.

In conclusion, coupled double-layer PCS Fano resonance filters with controlled lattice displacement have been investigated theoretically and experimentally, based on PDMS transfer printing technique and aligned EBL pattern processes. Theoretically, optical filter Q factors can approach  $2.11 \times 10^8$  or even higher. Experimentally, Q factors of 11 500 to 80 000 were demonstrated for the filters with simulated Q factors of 16 000 and 130 000, respectively. The results suggest this type of coupled bi-layer PCS structure can offer a platform for high Q optical filters, as well as platforms for optomechanics, reconfigurable optics, integrated photonics, and sensing systems.

The authors appreciate the support from US AFOSR under Grant Nos. FA9550-08-1-0337 and FA9550-09-1-0704, from ARO under Grant No. W911NF-09-1-0505, and from NSF under Grant No. ECCS-1308520.

<sup>1</sup>S. Fan and J. D. Joannopoulos, *Phys. Rev. B* **65**(23), 235112 (2002).

<sup>2</sup>R. Magnusson and S. S. Wang, *Appl. Phys. Lett.* **61**, 1022 (1992).

<sup>3</sup>Y. Kanamori, T. Kitani, and K. Hane, *Appl. Phys. Lett.* **90**, 031911 (2007).

<sup>4</sup>W. Suh and S. Fan, *Appl. Phys. Lett.* **84**, 4905 (2004).

<sup>5</sup>W. Zhou, Z. Ma, H. Yang, Z. Qiang, G. Qin, H. Pang, L. Chen, W. Yang, S. Chuwongin, and D. Zhao, *J. Phys. D* **42**, 234007 (2009).

<sup>6</sup>C. J. Chang-Hasnain, *Semicond. Sci. Technol.* **26**(1), 014043 (2011).

<sup>7</sup>H. Wu, W. Mo, J. Hou, D. Gao, R. Hao, H. Jiang, R. Guo, W. Wu, and Z. Zhou, *J. Opt.* **12**, 045703 (2010).

<sup>8</sup>H. Yang, D. Zhao, S. Chuwongin, J. H. Seo, W. Yang, Y. Shuai, J. Berggren, M. Hammar, Z. Ma, and W. Zhou, *Nat. Photonics* **6**(9), 615 (2012).

<sup>9</sup>C. Sciancalepore, B. B. Bakir, X. Letartre, J. Harduin, N. Olivier, C. Seassal, J. Fedeli, and P. Viktorovitch, *IEEE Photon. Technol. Lett.* **24**(6), 455 (2012).

<sup>10</sup>M. C. Y. Huang, Y. Zhou, and C. J. Chang-Hasnain, *Nat. Photonics* **1**(2), 119 (2007).

<sup>11</sup>V. Lousse, W. Suh, O. Kilic, S. Kim, O. Solgaard, and S. Fan, *Opt. Express* **12**(8), 1575 (2004).

<sup>12</sup>R. Magnusson and M. Shokoh-Saremi, *Opt. Express* **16**(5), 3456 (2008).

<sup>13</sup>A. E. Miroshnichenko, S. Flach, and Y. S. Kivshar, *Rev. Mod. Phys.* **82**(3), 2257 (2010).

<sup>14</sup>W. Suh, M. F. Yanik, O. Solgaard, and S. Fan, *Appl. Phys. Lett.* **82**(13), 1999 (2003).

<sup>15</sup>K. B. Crozier, V. Lousse, O. Kilic, S. Kim, S. Fan, and O. Solgaard, *Phys. Rev. B* **73**(11), 115126 (2006).

<sup>16</sup>C. Grillet, D. Freeman, B. Luther-Davies, S. Madden, R. McPhedran, D. J. Moss, M. J. Steel, and B. J. Eggleton, *Opt. Express* **14**(1), 369 (2006).

<sup>17</sup>L. Zhou and A. W. Poon, *Opt. Lett.* **32**(7), 781 (2007).

<sup>18</sup>H. Yang, Z. Qiang, H. Pang, Z. Ma, and W. D. Zhou, *Electron. Lett.* **44**(14), 858 (2008).

<sup>19</sup>Z. Qiang, H. Yang, L. Chen, H. Pang, Z. Ma, and W. Zhou, *Appl. Phys. Lett.* **93**, 061106 (2008).

<sup>20</sup>L. Chen, Z. Qiang, H. Yang, H. Pang, Z. Ma, and W. D. Zhou, *Opt. Express* **17**(10), 8396 (2009).

<sup>21</sup>W. Suh, O. Solgaard, and S. Fan, *J. Appl. Phys.* **98**, 033102 (2005).

<sup>22</sup>M. Notomi, H. Taniyama, S. Mitsugi, and E. Kuramochi, *Phys. Rev. Lett.* **97**(2), 023903 (2006).

<sup>23</sup>V. Liu, M. Povinelli, and S. Fan, *Opt. Express* **17**(24), 21897 (2009).

- <sup>24</sup>Y. Roh, T. Tanabe, A. Shinya, H. Taniyama, E. Kuramochi, S. Matsuo, T. Sato, and M. Notomi, [Phys. Rev. B](#) **81**(12), 121101 (2010).
- <sup>25</sup>Y. Shuai, D. Zhao, Z. Tian, J. Seo, D. V. Plant, Z. Ma, S. Fan, and W. Zhou, [Opt. Express](#) **21**(21), 24582 (2013).
- <sup>26</sup>J. A. Rogers, M. G. Lagally, and R. G. Nuzzo, [Nature](#) **477**(7362), 45 (2011).
- <sup>27</sup>K. Zhang, J. H. Seo, W. Zhou, and Z. Ma, [J. Phys. D](#) **45**(14), 143001 (2012).
- <sup>28</sup>V. Liu and S. Fan, [Comput. Phys. Commun.](#) **183**(10), 2233 (2012).
- <sup>29</sup>B. Luk'yanchuk, N. I. Zheludev, S. A. Maier, N. J. Halas, P. Nordlander, H. Giessen, and C. T. Chong, [Nature Mater.](#) **9**(9), 707 (2010).